

Jones, Dr. P. M. Richards, and Dr. B. G. Silbernagel.

*Work supported by the U. S. Atomic Energy Commission.

¹See, for example, A. Tucciarone, J. M. Hastings, and L. M. Corliss, *Phys. Rev. Lett.* **26**, 257 (1971).

²This work is part of a systematic study of nuclear relaxation in the rare-earth monophosphides. See, S. M. Myers and A. Narath, *Bull. Amer. Phys. Soc.* **16**, 315 (1971), and to be published.

³A. C. Switendick and E. D. Jones, *Bull. Amer. Phys. Soc.* **13**, 365 (1968); R. J. Gambino, D. E. Eastman, T. R. McGuire, V. L. Moruzzi, and W. D. Grobman, *J. Appl. Phys.* **42**, 1468 (1971).

⁴G. Busch, P. Schwob, and O. Vogt, *Phys. Lett.* **11**, 100 (1964).

⁵E. D. Jones, *Phys. Rev.* **180**, 455 (1969).

⁶E. D. Jones and B. Morosin, *Phys. Rev.* **160**, 451 (1967); note that the value of the Curie-Weiss temperature has been revised in Ref. 5 to -22.4°K . The exchange ratio of 4 given in the text comes from using the latter value in the molecular-field analysis.

⁷See, for example, C. P. Slichter, *Principles of Magnetic Resonance* (Harper & Row, New York, 1963), Chap. 5.

⁸E. L. Hahn, *Phys. Rev.* **80**, 580 (1950).

⁹In the high-field limit, T_1^{-1} is anisotropic with respect to field direction, so that taking a powder average leads to a nonexponential recovery of the total nuclear magnetization. The value used here corresponds to the initial slope of the recovery, and therefore is the average value of the relaxation rate.

¹⁰See, for example, J. E. Gulley, D. Hone, D. J. Scalapino, and B. G. Silbernagel, *Phys. Rev. B* **1**, 1020 (1970), and references therein.

¹¹Gulley, Hone, Scalapino, and Silbernagel, Ref. 10.

Parametric Excitation in the Ionosphere

A. Y. Wong and R. J. Taylor

TRW Systems, Redondo Beach, California 90278

(Received 19 July 1971)

Parametric excitation of ion waves is invoked to explain the efficient interaction between electromagnetic waves and the ionosphere.

We wish to report the parametric excitation of ion waves in the ionosphere by irradiation with an electromagnetic wave at the characteristic electron frequency for the desired height. When an electromagnetic wave ($\omega_0, k_0 \approx 0$) is incident upon the ionosphere it can stimulate the emission of an ion mode of ω_i and k_i if an electron mode of ω_e and k_e is emitted such that $\omega_0 = \omega_e + \omega_i$ and $\vec{k}_0 = \vec{k}_e + \vec{k}_i$. In the ionosphere where the gradient is gentle, the ion wave facilitates the coupling between the long-wavelength electromagnetic wave and the electrostatic electron wave of much shorter wavelength. The excited ion wave ω_i can be either a purely growing mode¹ ($\text{Re}\omega_i = 0, k_i \neq 0$, the nonoscillatory parametric instability) or a propagating ion acoustic mode² ($\omega_i = \alpha k_i v_{i\text{th}}$, the oscillatory parametric decay instability). For $T_e \approx T_i$ these two processes have approximately the same thresholds and can occur simultaneously. A consequence of this parametric coupling is that electrostatic electron waves are excited *at* and *below* the electromagnetic frequency ω_0 as dictated by the frequency-matching condition. Indeed, the intercoupling between electron and ion modes establishes a complementarity between the behaviors

of these two sets of modes of vastly different frequencies and properties.

Since the intercoupling between ω_0 and ω_i enhances ω_e (and the same holds for the interaction between ω_0 and ω_e) the parametric coupling process possesses a built-in feedback enhancement; such enhancement indeed has been demonstrated for low-frequency ion waves in which one drift wave externally driven decays into two lower-frequency drift waves.³

The efficiency of the parametric coupling between an electromagnetic pump near ω_p , the plasma frequency, and an ion acoustic wave has been theoretically predicted to have a minimum excitation power at $T_e \approx T_i$ given by²

$$P_0 = c \frac{E_0^2}{8\pi} = c 8n_e k T_e \frac{\gamma_e}{\omega_p} \frac{\gamma_i}{\omega_i}, \quad (1)$$

where γ_i, γ_e are the damping of the ion wave and the electron plasma wave, respectively, n_e is the electron density, and $\omega_i = k_i [(k T_e + k T_i / M_i)]^{1/2}$ is ion acoustic wave frequency. We note that the parametric threshold depends on both the electron and ion damping. The threshold power can be considerably reduced if $\gamma_e \ll \omega_p$.

We wish to present preliminary data from ex-

periments which have been planned with the above theoretical ideas in mind. Ionospheric conditions (usually daytime conditions) were chosen such that photoelectron fluxes were at a maximum in order that optimum coupling between electron and ion modes can take place.⁴

In this experiment the method of investigating the excited ion waves utilizes the fact that the spectrum of the excited electron plasma oscillations reflects the presence of parametrically excited ion waves. A high-frequency (hf) wave (5.62 MHz, $\lambda = 60$ m, 100 kW) corresponding to the plasma frequency ω_p , at a height of approximately 200 km is transmitted vertically by the Arecibo 1000-ft antenna⁵ (geomagnetic latitude, 30° N, magnetic shell number $L \approx 1.5$; geographic latitude, 18° N, longitude, 67° W) with an overall beam width of approximately 10°. The beam is circularly polarized in a direction unfavorable to the electron cyclotron rotation, commonly called the 0 mode. The excited plasma oscillation is detected as upper and lower sidebands in the Thomson back-scattering return of a 2-MW radar at 430 MHz ($\lambda = 0.70$ m and pulse width of 200 μ sec). In order to avoid extraneous signals, both the hf and the Thomson radar transmitters are turned off during the time the ionospheric return signal is monitored, as shown in Fig. 1(a). Under daytime conditions which include the sunlit periods of the conjugate points (50° S latitude,

67° W longitude) where photoelectrons are believed to exist, the upper sideband at 435.62 MHz is so strong, sometimes exceeding 12000°K in radiation temperature, that a direct monitoring on the scope is possible as shown in Fig. 1(b). The direct monitoring technique permits us to investigate the decay of the electron plasma waves and the dependence of the amplitude of the plasma waves as function of the incident power within the order of minutes, before ionospheric conditions could change.

The lower sideband at 424.38 MHz is observed to have in general a lower amplitude (approximately by a factor of 3). The upper sideband corresponds to the scattering by electron plasma waves traveling from south to north whereas the lower sideband corresponds to waves traveling in the opposite direction. For the period of the experiment (January) it is quite likely that the net photoelectron flux flowed preferably toward the north. This could explain the greater enhancement in the upper sideband. We shall limit our following discussions to the characteristics of the upper sideband.

At the maximum available incident power of 30 μ W/m², the line shape of the upper sideband is examined using a narrow bandwidth of 10 kHz in the receiver. By successively shifting the receiver frequency, the upper sideband was observed to be highly asymmetric as shown in Fig. 2. The downward frequency spread around the upper sideband (435.62 MHz) extends to 30 kHz, the order of the ion plasma frequency. This asymmetric line shape appears to support our parametric-coupling model in which the incident electromagnetic mode decays into an electron mode and an ion mode. In a parallel

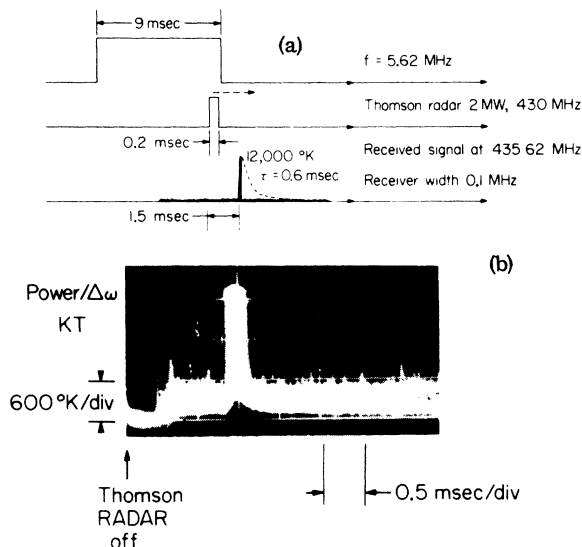


FIG. 1. (a) Timing sequence showing the hf radiation pulse (5.62 MHz) with maximum power at 100 kW, the Thomson radar pulse, and the ionospheric return received at the shifted frequency (435.62 MHz). (b) The typical observation of the return of the upper sideband at 435.62 MHz on the scope under daytime conditions.

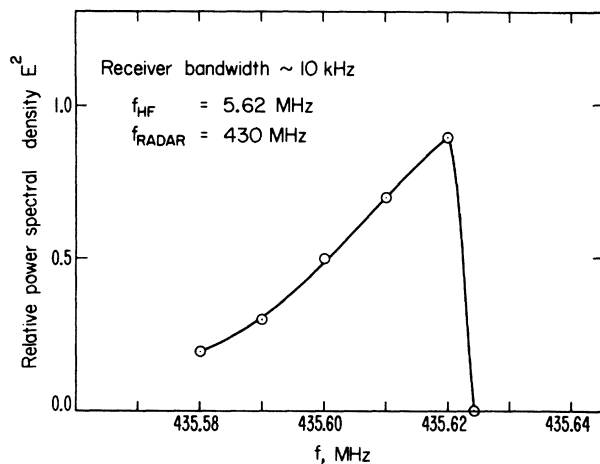


FIG. 2. Line shape of the upper sideband at 435.62 MHz.

laboratory experiment⁶ this asymmetric line shape (downward spread $\Delta\omega$) is accompanied by a corresponding increase in the ion fluctuations over the same frequency range $\Delta\omega$.

By delaying the Thomson radar with respect to the hf pulse, as shown by the dashed line in Fig. 1(a), the plasma wave was found to have an e -fold decay time of 0.6 msec. This measured damping rate enables us to estimate the minimum power required by the parametric theory, Eq. (1). This damping time is shorter than the electron-neutral collision time (≈ 2 msec).

At a given power of the incident hf electromagnetic wave, the energy density of the excited plasma wave is proportional to the received power in the sideband (435.62 MHz) of the Thomson radar. For the long pulse employed in our experiments the electron plasma wave is assumed to reach steady state, and its amplitude is determined by the excitation and the saturation mechanisms. By varying the hf transmitter power we observed a nonlinear dependence of the energy density $E_L^2(\omega_p)$ of the excited longitudinal plasma waves on the power density E_{hf}^2 of the high-frequency electromagnetic wave at 5.62 MHz evaluated at the height of interaction (≈ 200 km) as shown in Fig. 3.

Significant enhancement of the plasma wave was observed to start at a power of $10 \mu\text{W}/\text{m}^2$, and the energy density of the electron plasma line continued to increase up to the maximum available power density. Considering the damping rate γ_e of the electron plasma oscillation in Eq. (1) as given by the inverse of the measured decay time 0.6 msec, and using a mean electron temperature of 0.2 eV and $\gamma_i/\omega_i \approx 1$ as appropriate

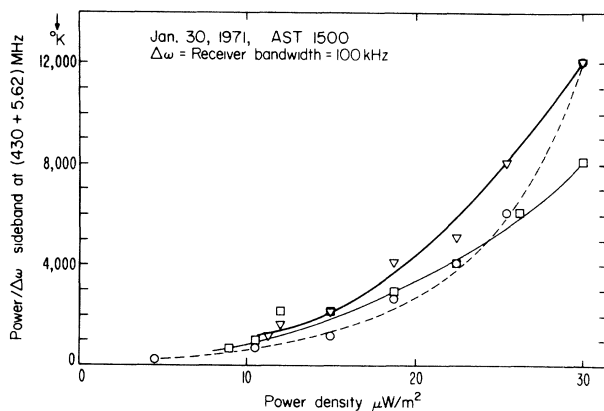


FIG. 3. Determination of threshold for the upper sideband at 435.62 MHz in three runs taken within 10 min. The changing ionospheric conditions are believed to be responsible for the nonreproducibility.

for $T_e/T_i \approx 1$, we obtain from Eq. (1) a threshold value of $1 \text{ mW}/\text{m}^2$. This theoretical minimum power is further reduced by the enhancement of the incident electromagnetic field as it approaches the cutoff-layer altitude h where $\omega_p(h) = \omega_0$ due to a reduction in its group velocity. A number of authors⁷ have shown that the incident field is enhanced for our own present experimental conditions by $A(L, \lambda_0) \approx 10$, where L is the scale height and λ_0 the free-field space wavelength. The required input power is correspondingly reduced by $A^2 \approx 10^2$. The overall theoretical consideration yields a minimum power of $10 \mu\text{W}/\text{m}^2$, in reasonable agreement with the observation.

We have inferred from our measurements of the line shape, the power dependence, and a consideration of the matching between incident electromagnetic and electrostatic waves that ion waves can be excited parametrically in the ionosphere by means of high-frequency electromagnetic waves matched to a characteristic electron frequency. Supported by our laboratory experiments,⁸ this scheme promises a new active interaction with the ionosphere. A common method of measuring electron and ion temperatures in the ionosphere has been to monitor the frequency spread around the main Thomson radar return, enhanced ion lines at $\Delta\omega = 2k_T v_i$ (k_T is the wave number of the Thomson radar) being interpreted as a rise in T_e/T_i . The present interpretation, showing that the ion lines can be independently enhanced by nonlinear coupling from electron plasma modes *without* an accompanying increase in T_e/T_i , could modify the usual straightforward interpretation in terms of temperature rise.

The authors are particularly grateful to Dr. W. E. Gordon for the very fine Thomson and hf radar facilities used in their measurements. The data were taken directly on scope with the very kind cooperation of Dr. H. Carlson and Mr. R. Showen. We wish to acknowledge assistance from the technical personnel at the Arecibo facility, in particular Mr. F. Harris. Finally, we wish to express our thanks to Dr. D. Arnush, Dr. B. D. Fried, and Dr. C. F. Kennel of TRW Systems and to Dr. F. Perkins of Princeton University for theoretical discussions concerning the experiment.

¹K. Nishikawa, J. Phys. Soc. Jap. 24, 916, 1152 (1968); P. Kaw and J. M. Dawson, Phys. Fluids 12, 2586 (1969).

²D. F. DuBois and M. V. Goldman, Phys. Rev. **164**, 207 (1967).

³A. Y. Wong, M. V. Goldman, F. Hai, and R. Rowberg, Phys. Rev. Lett. **21**, 518 (1968); F. Hai and A. Y. Wong, Phys. Fluids **13**, 672 (1970).

⁴The parametric process is initiated by the coupling between thermal fluctuations and the incident pump; the results of parametric excitation are much stronger if nonequilibrium situations exist which cause enhanced fluctuations [see, e.g., F. F. Perkins, E. E. Salpeter, and K. O. Yngvesson, Phys. Rev. Lett. **14**, 579 (1965)]. Electron plasma waves can be generated by the fast electrons via a Cherenkov process at a rate greater than the Landau damping rate. As a result the level of plasma fluctuations is much enhanced above the thermal level. In addition the internal field is also enhanced by the plasma dielectric constant which con-

tains such a high-energy tail.

⁵W. E. Gordon and L. M. LaLonde, IRE Trans. Antennas Propagat. **9**, 17 (1961).

⁶R. Stenzel, UCLA Plasma Physics Group Report No. R-83, 1961 (unpublished).

⁷V. L. Ginzburg, *The Propagation of Electromagnetic Waves in Plasmas* (Gordon and Beach, New York, 1962); F. Perkins and P. Kaw, Princeton University Plasma Physics Laboratory Report No. MATT-812, 1970 (unpublished); D. Arnush, B. D. Fried, and C. F. Kennel, TRW Systems Group Report No. 3, 1971 (unpublished).

⁸A. Y. Wong, D. R. Baker, and N. Booth, Phys. Rev. Lett. **24**, 804 (1970); A. Y. Wong, D. Arnush, B. D. Fried, C. F. Kennel, R. J. Taylor, and N. Booth, TRW Systems Group Research Report No. 99900-7491-RO-00, 1970 (unpublished).

Ordering Transitions in Helium Monolayers*

Michael Bretz and J. G. Dash

Department of Physics, University of Washington, Seattle, Washington 98105

(Received 26 April 1971)

He³ and He⁴ monolayers on graphite at coverages $0.45 \leq x \leq 0.61$ show strong heat-capacity peaks near 3°K. Temperature dependences and densities indicate that both isotopes undergo second-order transitions from the two-dimensional gas state to a regular lattice in registry with the substrate structure.

A current study of helium monolayers adsorbed on graphite discloses several remarkable features not seen in films adsorbed on other substrates.¹ The heat capacities of both isotopes at low fractional coverages $0.14 \leq x \leq 0.4$ have been interpreted as indicating quantum degeneracy of two-dimensional (2D) gases in weak lateral fields due to substrate inhomogeneities.² In the present Letter we report results at somewhat higher coverages, where the appearance of novel characteristics are suggestive of order-disorder transitions.

The present measurements were made in the same apparatus as those previously reported, on samples having monolayer densities in the range $0.45 \leq x \leq 0.66$. Fractional coverages $x \equiv N/N_m$, where N_m is the He³ monolayer capacity $90 \text{ cm}^3 \text{ STP}$ obtained from a vapor pressure isotherm at 4.2°K.

Results are presented in Figs. 1 and 2, which compare He³ and He⁴ at three nearly equal coverages. The data show qualitative features indicating a regime distinct from that at lower x . The transition between regimes is evident in Fig. 1(a), which displays peaks for both isotopes at about 3°, while near 1° there are remnants of

the isotopically distinct "quantum-degeneracy" characteristics of lower-coverage films. As x is increased, the degeneracy characteristics are further suppressed, while the 3° peaks increase in area.

The appearance of the sharp He⁴ peak in Fig. 2 is suggestive of a second-order phase transition, and therefore we examined the data according to the power law³ $C = a|\epsilon|^{-\alpha} + b$, where $\epsilon = (T - T_c)/T_c$. We found that the data could be described over at least one decade of ϵ by a wide range of exponents, $0.1 \leq \alpha \leq 0.4$, while $2.92^\circ \leq T_c \leq 2.94^\circ$. For $\alpha = 0.3$, $T_c = 2.936^\circ$, the agreement extends to $\epsilon \approx 0.25$, considerably greater than the generally accepted range of critical behavior. However, since the role of low-lying fluctuations is known to be greater in 2D than in 3D systems, the critical region may be as wide as indicated. For the limiting value $\alpha \rightarrow 0$ the power law becomes logarithmic, as shown in Fig. 3. The choice $T_c = 2.927^\circ$ gave parallel lines for the low- and high-temperature regions, displaced by about $0.3k$. Kadanoff *et al.*³ discuss the uncertainties in extracting empirical coefficients from data over limited ranges of ϵ . It is clear that we have not explored the peak in

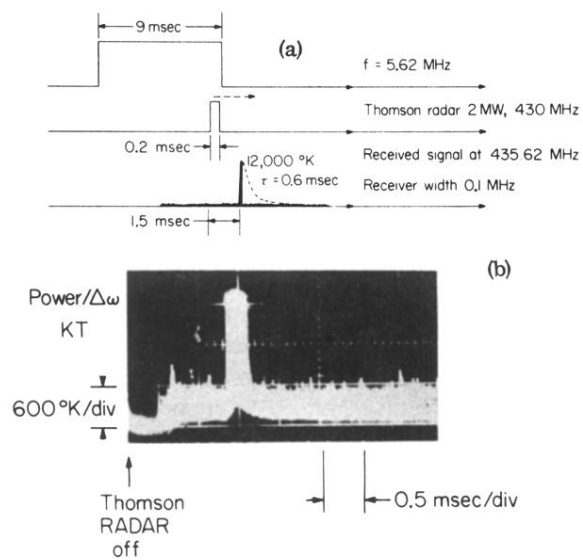


FIG. 1. (a) Timing sequence showing the hf radiation pulse (5.62 MHz) with maximum power at 100 kW, the Thomson radar pulse, and the ionospheric return received at the shifted frequency (435.62 MHz). (b) The typical observation of the return of the upper sideband at 435.62 MHz on the scope under daytime conditions.